

UCLA

UCLA Previously Published Works

Title

Molecular Signature of Antibody-Mediated Chronic Vasculopathy in Heart Allografts in a Novel Mouse Model

Permalink

<https://escholarship.org/uc/item/8xx8s1tm>

Journal

American Journal Of Pathology, 192(7)

ISSN

0002-9440

Authors

Tsuda, Hidetoshi
Dvorina, Nina
Keslar, Karen S
[et al.](#)

Publication Date

2022-07-01

DOI

10.1016/j.ajpath.2022.04.003

Peer reviewed



ELSEVIER

See related Commentary on page 986

CARDIOVASCULAR, PULMONARY, AND RENAL PATHOLOGY

Molecular Signature of Antibody-Mediated Chronic Vasculopathy in Heart Allografts in a Novel Mouse Model



Hidetoshi Tsuda,^{*} Nina Dvorina,^{*} Karen S. Keslar,^{*} Jessica Nevarez-Mejia,[†] Nicole M. Valenzuela,[†] Elaine F. Reed,[†] Robert L. Fairchild,^{*} and William M. Baldwin 3rd^{*}

From the Department of Inflammation and Immunity,^{*} Lerner Research Institute, Cleveland Clinic, Cleveland, Ohio; and the UCLA Immunogenetics Center,[†] Department of Pathology and Laboratory Medicine, David Geffen School of Medicine, University of California, Los Angeles, California

Accepted for publication
April 14, 2022.

Address correspondence to
William M. Baldwin 3rd, M.D.,
Ph.D., or Robert L. Fairchild,
Ph.D., Department of Inflammation
and Immunity, Lerner
Research Institute, Cleveland
Clinic, Cleveland, OH 44195.
E-mail: baldwiw@ccf.org or
fairchr@ccf.org.

Cardiac allograft vasculopathy (CAV) limits the long-term success of heart transplants. Generation of donor-specific antibodies (DSAs) is associated with increased incidence of CAV clinically, but mechanisms underlying development of this pathology remain poorly understood. Major histocompatibility complex–mismatched A/J cardiac allografts in B6.CCR5^{-/-} recipients have been reported to undergo acute rejection with little T-cell infiltration, but intense deposition of C4d in large vessels and capillaries of the graft accompanied by high titers of DSA. This model was modified to investigate mechanisms of antibody-mediated CAV by transplanting A/J hearts to B6.CCR5^{-/-} CD8^{-/-} mice that were treated with low doses of anti-CD4 monoclonal antibody to decrease T-cell–mediated graft injury and promote antibody-mediated injury. Although the mild inhibition of CD4 T cells extended allograft survival, the grafts developed CAV with intense C4d deposition and macrophage infiltration by 14 days after transplantation. Development of CAV correlated with recipient DSA titers. Transcriptomic analysis of microdissected allograft arteries identified the Notch ligand *Dll4* as the most elevated transcript in CAV, associated with high versus low titers of DSA. More importantly, these analyses revealed a differential expression of transcripts in the CAV lesions compared with the matched apical tissue that lacks large arteries. In conclusion, these findings report a novel model of antibody-mediated CAV with the potential to facilitate further understanding of the molecular mechanisms promoting development of CAV. (*Am J Pathol* 2022, 192: 1053–1065; <https://doi.org/10.1016/j.ajpath.2022.04.003>)

The success of heart transplantation to treat end-stage cardiac disease is undermined by the development of chronic allograft vasculopathy (CAV). More than 50% of heart grafts develop CAV within 5 years after transplantation.^{1–3} The arterial lesions consist of concentric intimal expansion with proliferating myofibrocytes and mononuclear cell infiltrates of T cells and macrophages, resulting in narrowing of the graft arterial lumen, decreased blood flow, and graft tissue ischemia.^{4,5} Mechanisms underlying the initiation and progression of CAV remain unclear, and it is likely that multiple pathways of graft endothelial cell–mediated injury initiate and promote CAV. Development of CAV is often associated with donor-specific antibody (DSA) to allogeneic human leukocyte

antigen molecules in the serum of heart transplant recipients, suggesting that some forms of CAV are initiated and exacerbated by DSA binding to allograft major histocompatibility complex (MHC) targets expressed by the arterial endothelial cells of the graft.^{6–8} Antibodies to MHC molecules can have direct effects on endothelial cells by provoking activation of the complement cascade to mediate

Supported by NIH National Institute of Allergy and Infectious Diseases grants R01 AI135201-01A1 (H.T., N.D., J.N.-M., N.M.V., E.F.R., R.L.F., and W.M.B.) and PO1 AI087586 (H.T., N.D., R.L.F., and W.M.B.) and by the Clinical Trials in Organ Transplantation NanoString Core, supported by U01 AI063594 (K.S.K. and R.L.F.).

R.L.F. and W.M.B. contributed equally as senior authors.
Disclosures: None declared.

endothelial cell injury.^{9,10} These antibodies can also stimulate the activation of endothelial cells to proliferate, express cell adhesion molecules, and produce inflammatory cytokines, including chemoattractant cytokines directing macrophage infiltration into CAV lesions, which correlates with clinical antibody-mediated rejection of heart allografts.^{11–18}

Several preclinical models have been developed that examine the role of T cells in heart allograft CAV. One commonly used mouse model involves the transplantation of hearts from *H-2^{bm12}* donors to C57BL/6 mice, a single class II MHC disparity.^{19,20} The heart grafts develop CAV over the course of 30 to 60 days, which is dependent on the activation of *bm12*-reactive CD4 T cells. This donor-reactive T-cell response and the class II MHC disparity are restricted to a three amino acid difference in the peptide binding groove of *I-A^{bm12}*, suggesting that effector functions expressed by the reactive CD4 T cells mediate the development of CAV. Similarly, peptides from minor histocompatibility antigens, such as the male HY antigen, can cause T-cell-mediated chronic rejection of heart allografts.^{21,22} Using this model, CD4 T cells were found to orchestrate intense macrophage infiltrates in the interstitium and arteries of the graft, but the transcriptome profile for the infiltrates in the CAV lesions was distinctly different from that in the interstitium.²¹

Evidence for antibody-mediated CAV in preclinical heart allograft models has been provided by transfer of monoclonal antibodies specific for graft class I MHC to immunodeficient heart allograft recipients, where the graft-reactive antibodies provoke CAV.^{23,24} Previous studies show a dysregulation of DSA responses to solid organ transplants in *CCR5^{-/-}* recipients, where complete MHC-mismatched solid organ allografts induce DSA titers with >40-fold increases than those induced in wild-type C57BL/6 recipients. *B6.CCR5^{-/-}* recipients reject MHC incompatible A/J cardiac allografts acutely between 7 and 8 days, independently of CD8 T cells.^{25,26} Herein, analysis of the histopathology of the rejecting heart allografts demonstrated acute arterial inflammation with endothelial injury and intense deposition of C4d. These initial studies led us to hypothesize that administering low doses of anti-CD4 T-cell monoclonal antibody (mAb) to *B6.CCR5^{-/-}CD8^{-/-}* mice at and for a short time after transplantation with complete MHC mismatched heart allografts would delay DSA production and prevent acute rejection. This would allow for the development of DSA-induced CAV and the identification of molecular transcript signatures specifically associated with the arterial lesions that are not expressed elsewhere in the graft tissue.

Materials and Methods

Mice

C57BL/6 (H-2^b), *B6.CCR5^{-/-}*, *B6.CD8^{-/-}*, and A/J (H-2^a) mice were purchased from the Jackson Laboratory (Bar

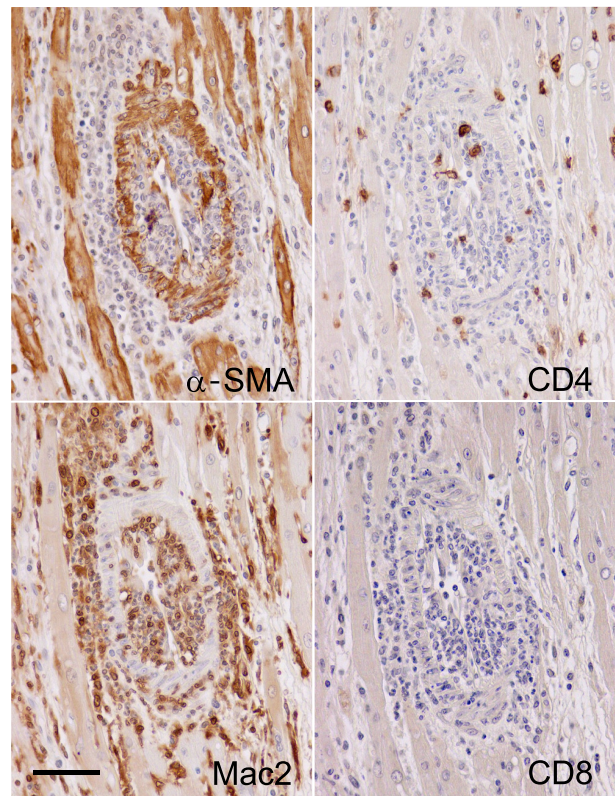


Figure 1 Near complete arterial occlusion due to neointima expansion composed of macrophages and α -smooth muscle actin expressing myofibrocytes with only scattered CD4 T cells. *B6.CCR5^{-/-}CD8^{-/-}* recipients of A/J cardiac allografts were treated with 100 μ g anti-CD4 monoclonal antibody on days 0, 2, 7, and 14. Terminal graft rejection at 35 days was characterized by near complete occlusive neointima expansion. Immunohistologic markers for α -smooth muscle actin (α -SMA) stained myofibrocytes in the intima, smooth muscle cells in the arterial media, and necrotic cardiomyocytes that lost visible cross-striations. Mac2 antibody stained profuse infiltrates of macrophages in the neointima, periarterial adventitia, and interstitium. Scattered CD4 T cells and no CD8 T cells were detected in the neointima. Scale bar = 50 μ m.

Harbor, ME), and *B6.CCR5^{-/-}* and *B6.CD8^{-/-}* mice were crossed to generate *B6.CCR5^{-/-}CD8^{-/-}* mice. All animal studies were conducted using male donor and recipient mice between 8 and 12 weeks of age, and all procedures using mice were approved by the Institutional Animal Care and Use Committee of the Cleveland Clinic (Cleveland, OH).

Heterotopic Cardiac Transplantation

Heterotopic vascularized cardiac transplantation was performed, as previously described.^{25,26} Briefly, complete MHC-mismatched A/J (H-2^a) hearts were transplanted to *B6.CD8^{-/-}* or *B6.CCR5^{-/-}CD8^{-/-}* mice on a C57BL/6 background (H-2^b). Hearts from C57BL/6 were transplanted to *B6.CCR5^{-/-}CD8^{-/-}* recipients as isograft controls. Where indicated, recipients were treated intraperitoneally on days 0, 2, and 7 after transplant with anti-CD4 mAb (100 μ g of a 1:1 cocktail of YTS191 and GK1.5; Bio X Cell, Lebanon, NH). To deplete B cells and prevent DSA

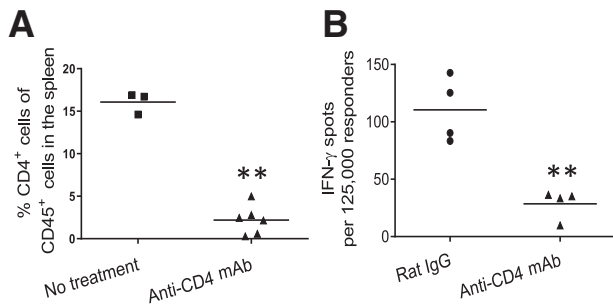


Figure 2 Depletion of CD4 T cells in B6.CCR5^{-/-}CD8^{-/-} recipients of A/J cardiac allografts. B6.CCR5^{-/-}CD8^{-/-} recipients of A/J cardiac allografts were untreated, or treated with 100 μg control rat IgG or anti-CD4 monoclonal antibody (mAb) on days 0, 2, and 7 after transplant. On day 10, the presence of CD4 T cells in the recipient spleen was assessed by flow cytometry (A) and ELISPOT enumeration (B) of donor-reactive CD4 T cells producing interferon (IFN)-γ. ***P* < 0.01 versus control rat IgG-treated recipients.

production, B6.CCR5^{-/-}CD8^{-/-} and, as a control, B6.CD8^{-/-} recipients were treated intraperitoneally with 0.25 mg anti-mouse CD20 mAb (AISB12; Bio X Cell) on either days -2 and 6 or days -2, 3, and 8 after transplantation, as previously reported.²⁷ Grafts were monitored daily for beating by recipient abdominal palpation and were recovered on day 14 after transplant for analyses.

Donor-Specific Antibody Quantitation by Flow Cytometry

Flow cytometry was performed to quantitate DSA in non-recipient and cardiac graft recipient serum, as previously reported.²⁶ Briefly, aliquots of donor strain A/J thymocyte suspensions were incubated with serial dilutions of recipient sera recovered at defined time points after transplant. After 60 minutes, the cells were washed and stained with fluorescein isothiocyanate-conjugated goat anti-mouse IgG, Fcγ fragment-specific mAb (Jackson ImmunoResearch, West Grove, PA). The geometric mean fluorescence intensity of each dilution of each serum sample was determined, and the dilution that returned the geometric mean fluorescence intensity to the background level observed when B6 thymocytes were stained with autologous wild-type B6 serum was divided by two and reported as the titer.

Flow Cytometry

To verify CD4 T depletion in B6.CCR5^{-/-}CD8^{-/-} heart allograft recipients treated with 100 μg control rat IgG or anti-CD4 mAb on days 0, 1, and 7, recipients were sacrificed on day 14 after transplant, single-cell suspensions from the spleen were prepared, and aliquots were stained with fluorescein isothiocyanate-conjugated anti-CD45 mAb (30-F111; BD Biosciences, San Jose, CA) and phosphatidylethanolamine-conjugated anti-CD4 mAb (RM4-5; BD Biosciences) and run on an LSRII flow

cytometer (BD Biosciences) followed by data analyses using FlowJo software version 10 (Tree Star Inc., Ashland, OR).

ELISPOT Analysis of Heart Allograft Donor-Reactive CD4 T Cells Producing IFN-γ

ELISPOT assays to enumerate donor-reactive CD4 T cells producing interferon (IFN)-γ were performed, as previously reported, using IFN-γ capture and detecting anti-mouse IFN-γ mAb from BD Biosciences.²⁵ Briefly, B6.CCR5^{-/-}CD8^{-/-} heart allograft recipients were treated with 100 μg control rat IgG or anti-CD4 mAb on days 0, 1, and 7; recipients were sacrificed on day 10 after transplant; and single-cell suspensions from the spleen were prepared and aliquots were co-cultured with mitomycin C-treated A/J spleen cells in serum-free CTL-Test medium (Cellular Technology Ltd, Cleveland, OH) supplemented with 1 mmol/L L-glutamine. After 24 hours, the cells were removed by washing with phosphate-buffered saline/0.05% Tween 20, and the filters were developed to detect IFN-γ. The resulting spots were analyzed using an ImmunoSpot Series analyzer version 5 (Cellular Technology Ltd).

Pathologic Assessment of Heart Grafts

Recovered heart grafts were fixed by immersion in methanol/acetic acid, embedded in paraffin block, and cut into sections (5 μm thick) for immunohistochemistry analyses. After antigen retrieval and paraffin removal with Trilogy (Cell Marque, Hot Springs, AR) in a pressure cooker, endogenous peroxidase activity was quenched with 0.03% H₂O₂ for 10 minutes, and non-specific protein interactions were inhibited by incubation with serum-free protein block (Dako, Carpinteria, CA). The slides were then stained with the following primary antibodies: monoclonal rat antibody to mouse Mac2 (Cedarlane Laboratories, Burlington, NC), rabbit monoclonal anti-CD4 antibody (Abcam, Cambridge, MA), rabbit polyclonal antiserum to α-smooth muscle actin (Abcam), and rabbit polyclonal anti-serum to mouse C4d, produced as described previously.²⁸ Primary antibodies were visualized using rat or rabbit on mouse HRP-Polymer Kits (Biocare Medical, Concord, CA), followed by diaminobenzidine and counterstained with hematoxylin. Slides were viewed by light microscopy, and images were captured using ImagePro Plus (Media Cybernetics, Silver Springs, MD).

RNA Isolation from Heart Grafts for Real-Time Quantitative PCR Analysis

RNA was isolated from heart isografts and allografts using Fibrous Tissue kits (Qiagen, Valencia, CA) and reverse transcribed using the High-Capacity cDNA Reverse Transcription Kit (Applied Biosystems, Thermo Fisher Scientific, Waltham, MA), as previously described.²⁵ Synthesized cDNA was used for quantitative PCR with TaqMan Fast

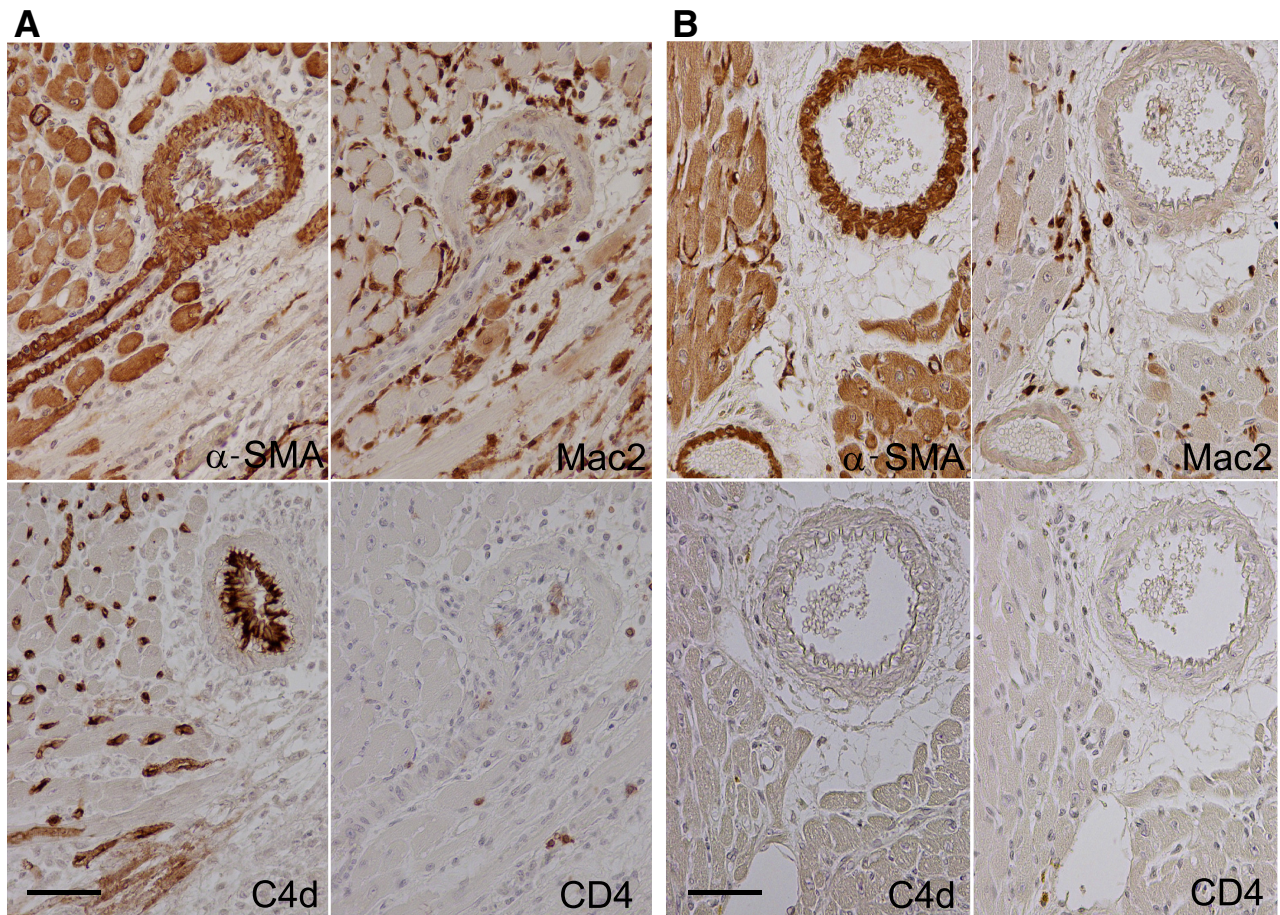


Figure 3 Cardiac grafts in anti-CD4 monoclonal antibody (mAb)-treated B6.CCR5^{-/-}CD8^{-/-} recipients. **A:** A/J cardiac allografts in B6.CCR5^{-/-}CD8^{-/-} recipients treated with 100 μ g anti-CD4 mAb on days 0, 2, and 7 display early manifestations of chronic arteriopathy 14 days after transplantation. Myofibrocytes in the intima and smooth muscle cells in the media of the large artery with a smaller arterial branch were stained by antibodies to α -smooth muscle actin (α -SMA). Mac2 antibody stained moderate numbers of macrophages in the neointima, periarterial adventitia, and interstitium. Scattered interstitial CD4 T cells were detected. Intense linear deposits of C4d line the arterial and capillary endothelium. **B:** B6 cardiac isografts in B6.CCR5^{-/-}CD8^{-/-} recipients treated with 100 μ g anti-CD4 mAb on days 0, 2, and 7 display no evidence of chronic arteriopathy 14 days after transplantation. Smooth muscle cells in the media of the large artery upper right and smaller artery were stained by antibodies to α -SMA. No neointima was evident. Mac2 antibody stained scattered macrophages in the interstitium. Scattered interstitial CD4 T cells were detected. No deposits of C4d were detected on the arterial and capillary endothelium. Scale bar = 50 μ m (A and B).

Universal Master Mix (Applied Biosystems) and TaqMan primer sets (SH2D1B1; Mm04210368_m1, MYBL1; Mm00485327_m1, CX3CR1; Mm02620111_s1, MRPL32; and Mm00777741_sH). All PCRs were performed on a 7500 Fast Real-Time PCR System (Applied Biosystems) and quantified using the ddCt method and normalized to MRPL32 gene expression.

Laser Capture Microdissection and RNA Extraction for Nanostring Analysis

Heart allografts were embedded in OCT (Tissue-Tek; Miles Laboratories, Inc., Naperville, IL), cryosectioned (12 μ m thick), and mounted as serial cross-sections. Arteries in the heart allografts were microdissected, 25 to 30 sections from each of two grafts, with a Leica LMD7000 laser microdissection microscope (Leica Microsystems, Buffalo

Grove, IL); and pooled sections from each of the two grafts were collected in 0.5-mL RNase-free PCR tube caps with 75 μ L of RLT buffer from the RNeasy Micro kit (Qiagen, Valencia, CA). Total RNA was extracted using an RNeasy Fibrous Tissue Mini kit (Qiagen) for recovered grafts or an RNeasy Micro kit (Qiagen) for microdissected vessels, and was interrogated using the NanoString nCounter platform (NanoString Technologies, Inc., Seattle, WA) by hybridization to the mouse PanCancer Immune Panel. Raw counts were normalized and analyzed using advanced analysis on nSolver version 4.0 (NanoString Technologies, Inc.). To identify genes that were significantly differentially expressed, cutoffs of $P \leq 0.05$ were selected and defined at a threshold of a twofold change. The NanoString transcript expression data have been deposited in National Center for Biotechnology Information's Gene Expression Omnibus and are accessible through Gene Expression Omnibus series

Table 1 Evaluation of the Large Arteries at the Base of Individual Transplants

Specimen	CAV ⁺ versus total large arteries	CAV high score*	Mac2 in intima*	DSA titer
CCR5/CD8 h22	3 of 5	2	2	128
CCR5/CD8 h15	2 of 2	1	1	256
CCR5/CD8 h23	1 of 3	1	1	256
CCR5/CD8 h16	3 of 6	2	2	256
CCR5/CD8 h14	2 of 2	1	1	512
CCR5/CD8 h20	4 of 4	2	3	1024
CCR5/CD8 h24	5 of 5	3	2	1024
CCR5/CD8 h17	3 of 3	2	1	2048
CCR5/CD8 h18	4 of 5	1	1	2048
	27 of 35 (77%)	1.6	1.5	
2x mCD20 h3	1 of 4	1	1	128
2x mCD20 h4	1 of 4	1	1	128
2x mCD20 h5	1 of 2	1	2	
2x mCD20 h6	3 of 3	1	2	256
2x mCD20 h7	4 of 4	2	2	256
	9 of 15 (60%)	1.2	1.6	
3x mCD20 h9	1 of 7	1	1	16
3x mCD20 h8	1 of 7	1	2	32
3x mCD20 h11	1 of 8	1	2	32
3x mCD20 h10	0 of 8	0	1	64
	3 of 30 (10%)	0.8	1.5	
CD8ko h5	0 of 2	0	1	128
CD8ko h2	0 of 3	0	1	256
CD8ko h4	3 of 4	2	2	256
CD8ko h3	2 of 3	1	1	512
	5 of 12 (42%)	0.8	1.3	
mCD20 CD8ko h6	0 of 5	0	0	32
mCD20 CD8ko h7	0 of 5	0	1	64
	0 of 10 (0%)	0.0	0.5	
B6-CCR5CD8 h10	0 of 2	0	0	4
B6-CCR5CD8 h11	0 of 3	0	0	4
B6-CCR5CD8 h6	0 of 3	0	0	8
B6-CCR5CD8 h7	0 of 2	0	0	8
B6-CCR5CD8 h8	0 of 3	0	0	8
B6-CCR5CD8 h9	0 of 2	0	0	8
	0 of 15 (0%)	0	0	

* α -Smooth muscle actin and Mac2 scored 0 to 3 in neointima: 0 indicates little or none; 1, <50% involvement; 2, >50% involvement; and 3, circumferential.

CAV, cardiac allograft vasculopathy; DSA, donor-specific antibody.

accession number GSE200623 (<https://www.ncbi.nlm.nih.gov/geo/query/acc.cgi?acc=GSE200623>).

Statistical Analysis

All data were analyzed using GraphPad Prism Pro version 10 (GraphPad Software Inc., San Diego, CA). All values are expressed as means \pm SEM. Comparisons between experimental and control or naïve groups for cellular infiltration and proliferation were determined by the nonparametric *U*-test, and *P* < 0.05 was considered to be statistically significant. Log2 normalized counts and expression ratios were generated using nSolver version 4.0 and advanced analysis 2.0 as well as ROSALIND analysis platform (NanoString Technologies, Inc.).

Results

Establishing a Model of CAV

B6.CCR5^{-/-}CD8^{-/-} recipients have been shown to produce markedly higher titers of DSA than wild-type recipients and acutely reject complete MHC incompatible A/J cardiac allografts between 7 and 8 days with intense deposition of C4d and endothelial injury.^{25,26} To delay this increased DSA production and prevent acute rejection, a series of preliminary experiments established that four doses of anti-CD4 mAb given intraperitoneally on days 0, 2, 7, and 14 after transplantation extended graft survival from 7 to 35 days. Complete rejection at day 35 after transplant was characterized by advanced CAV with near complete arterial

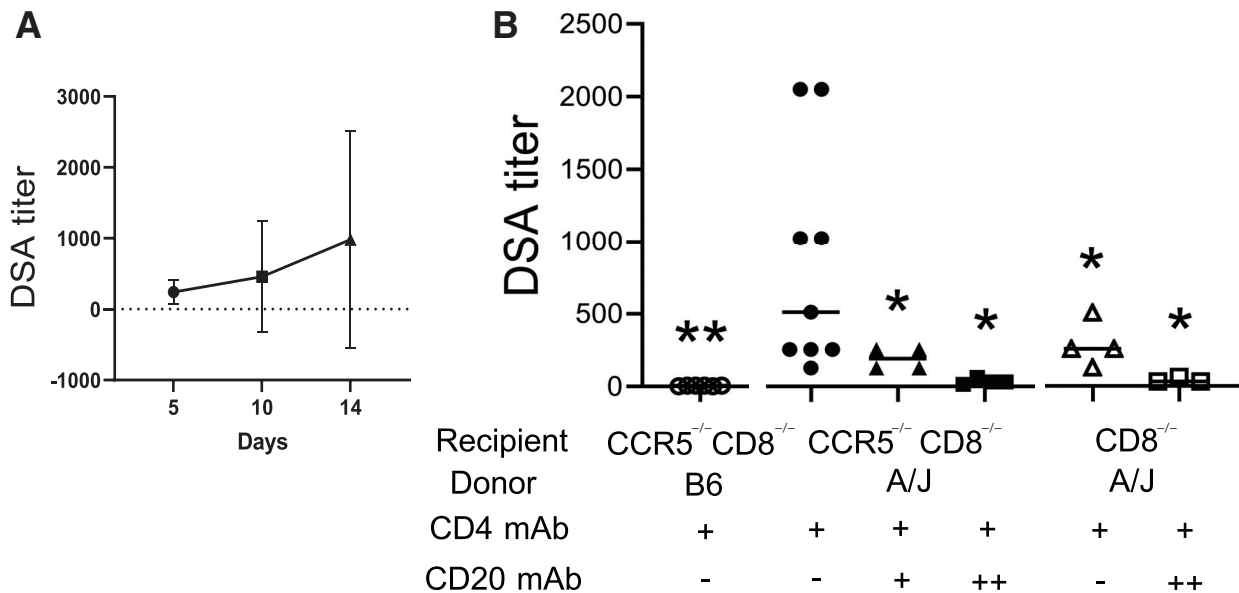


Figure 4 Donor-specific antibody (DSA) titers generated in response to A/J cardiac allografts. **A:** Increase of circulating IgG DSA in A/J allografts in B6.CCR5^{-/-}CD8^{-/-} recipients treated with three doses of 100 μ g/dose anti-CD4 monoclonal antibody (mAb) on days 0, 2, and 7 after transplant. **B:** Comparison of DSA in anti-CD4 mAb-treated isograft and allograft recipient groups on day 14 after transplant: B6 isografts to B6.CCR5^{-/-}CD8^{-/-} recipients; A/J allografts to B6.CCR5^{-/-}CD8^{-/-} recipients treated without or with two or three doses of anti-CD20 mAb; and A/J allografts to B6.CD8^{-/-} recipients treated without or with three doses of anti-CD20 mAb. **P* < 0.05, ***P* < 0.01 versus A/J allografts to B6.CCR5^{-/-}CD8^{-/-} recipients treated with anti-CD4 mAb.

occlusion due to neointima expansion composed of macrophages and α -smooth muscle actin expressing myofibrocytes with only scattered CD4 T cells (Figure 1).

To capture the early pathogenesis of chronic arteriopathy, B6.CCR5^{-/-}CD8^{-/-} recipients of A/J heart allografts were treated with anti-CD4 mAb on days 0, 2, and 7 after transplant, and graft arterial pathology was examined 14 days after transplantation. Analysis of graft recipient CD4 T cells on day 10 after transplant indicated decreased numbers of CD4 T cells in the spleen that was accompanied by marked decreases in donor-reactive T cells producing IFN- γ versus control non-treated or rat IgG-treated recipients (Figure 2). On day 14 after transplant, most allograft myocardium was viable and contained only moderate infiltrates of macrophages and scattered CD4 T cells (Figure 3A). However, early ischemic injury was evident in Gomori trichrome stain, with focal necrosis of individual myocytes and numerous vacuoles in viable myocytes²⁹ (Supplemental Figure S1). Evaluation of the large arteries at the base of nine individual transplants revealed that 77% (27/35) of the arteries had mild to moderate arteriopathy, characterized by concentric intimal expansion containing macrophages, α -smooth muscle actin expressing myofibrocytes, and intense C4d deposition (Table 1). Control isografts of B6 hearts into B6.CCR5^{-/-}CD8^{-/-} recipients treated with anti-CD4 mAb had no evidence of CAV (Table 1 and Figure 3B). In anti-CD4 mAb-treated B6.CCR5^{-/-}CD8^{-/-} recipients, the A/J heart allografts induced DSA that was detected at low titers on day 5 after transplant and increased to higher titers by day 14

(Figure 4A). Anti-CD4 mAb treatment only partially inhibited the IgG DSA titers induced by the allografts in B6.CCR5^{-/-}CD8^{-/-} recipients and resulted in a bimodal distribution of recipients with low or high titers (Figure 4B). The percentage of large arteries compromised by CAV also had a wide range but was correlated with the titer of DSA (Figure 5). In mice with DSA titers of 128 to 256, only about half of the arteries manifested CAV pathology (9/16), whereas CAV involved almost all large arteries (18/19) of allografts recovered from recipients with DSA titers of 512 to 2048 (Figure 5 and Table 1).

CAV Is Diminished in Recipients with Lower Titers of DSA

Two approaches were employed to further test the contribution of the high DSA titers to early CAV development. First, B6.CCR5^{-/-}CD8^{-/-} recipients were treated with B-cell depleting anti-mouse CD20 mAb on days -2 and 6. This treatment decreased day 14 after transplant DSA titers to 128 to 256 (Figure 4), and abated the severity and percentage of arteries (60%) per graft with CAV (Table 1). In this group, two recipients with lower DSA titers of 128 had few arteries with CAV (25%) and two recipients with higher titers of 256 had a higher percentage (5/7; 71%) of arteries with CAV (Table 1). More intensive anti-CD20 mAb administration to B6.CCR5^{-/-}CD8^{-/-} recipients on days -2, 3, and 8 after transplant further decreased the DSA titers and decreased CAV development and arterial inflammation in the allografts (Figures 4B and 6 and Table 1).

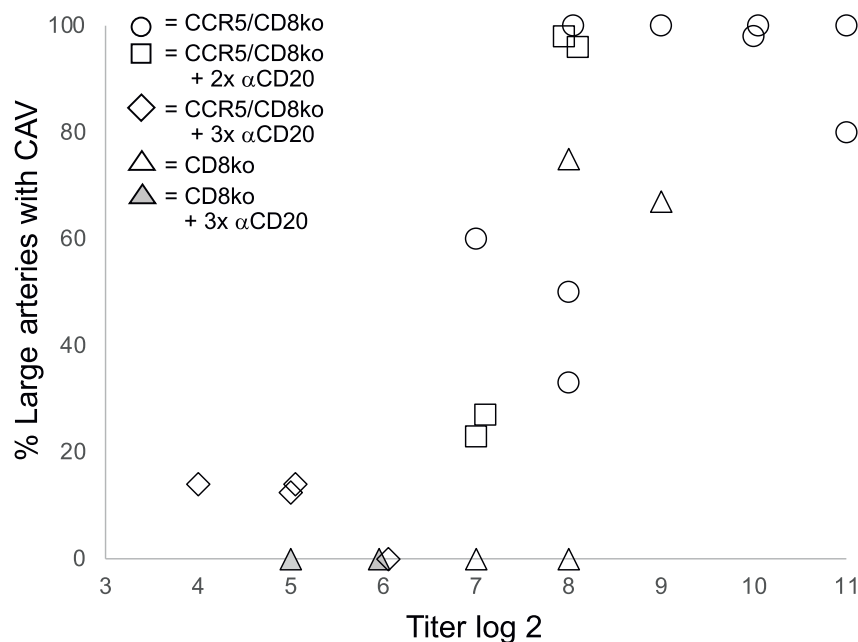


Figure 5 Scattergram showing correlation between donor-specific antibody (DSA) titers and percentage of large arteries with manifestations of cardiac allograft vasculopathy (CAV) in allograft recipients. Pearson regression analysis indicated $R^2 = 0.9827$ when comparing correlations between B6.CCR5^{-/-}CD8^{-/-} allograft recipients treated with versus without anti-mouse CD20 monoclonal antibody, indicating that >98% of the variance of the incidence of CAV in this model is explained by the DSA titer.

Second, the incidence of CAV in allografts from recipients that produce low titers of DSA was investigated by transplanting A/J hearts to B6.CD8^{-/-} mice. These recipients produced DSA titers of 128 to 512 (Figure 4B and Table 1). The pathologic findings in allografts to B6.CD8^{-/-} recipients manifested several key differences to allografts in B6.CCR5^{-/-}CD8^{-/-} recipients. First, there were more intense interstitial and periarterial infiltrates of macrophages in grafts from B6.CD8^{-/-} recipients compared with B6.CCR5^{-/-}CD8^{-/-} recipients (Figure 7). Second, the large arteries displayed evidence of acute injury, including infiltration of the media by clusters of macrophages and occasional CD4 T cells, as well as extensive endothelial cell injury, as manifested by swelling and detachment (Figures 6 and 7). This transmural arteritis contrasted with the CAV pathology in allografts from B6.CCR5^{-/-}CD8^{-/-} recipients with either high or low titers of DSA in which the arterial medium was intact and not infiltrated (Figures 1 and 3A). Treatment of B6.CD8^{-/-} allograft recipients with anti-CD20 mAb on days -2, 3, and 8 after transplant further decreased DSA titers and abrogated the development of CAV and graft arterial inflammation on day 14 (Figure 6).

Transcriptome Signature of Early CAV

To identify the transcriptome signature of CAV associated with high versus low titers of *de novo* DSA, arteries were microdissected from 25 to 30 sections of each of two allografts 14 days after transplantation to B6.CCR5^{-/-}CD8^{-/-} recipients. These were compared with microdissected arteries from two allografts recovered from B6.CCR5^{-/-}CD8^{-/-} recipients treated with anti-CD20 mAb to deplete B cells.

Multiplexed RNA detection was performed using nSolver analysis. Analysis of the data by both nCounter and Rosalind algorithms identified a consensus of eight transcripts that were increased greater than twofold with a $P < 0.05$ versus transcripts expressed by allograft arteries in allografts from recipients depleted of B cells (Figure 8A and Table 2). The most highly up-regulated of these genes was *Dll4* (delta-like canonical Notch ligand 4). The others included *Itga6* (a laminin receptor), *Abl1* (involved in cell differentiation and inflammatory functions of many leukocyte populations), *Cspg4* (involved in cell spreading on the endothelium basement membrane), and *Nfatc2* and *Trem2* (expressed in heart resident macrophages during inflammatory processes). In contrast, expression of six genes was decreased greater than twofold and with a $P < 0.05$ in the arterial lesions of allografts recovered from recipients with B cells and high DSA titers versus lesions of allografts recovered from recipients depleted of B cells and low DSA titers. These differentially expressed genes included those encoding chemokines that direct the recruitment of T cells and dendritic cells (*Ccl21*), endothelial cells (*Cxcl14*), monocytes (*Ccl7*), and genes associated with promotion of antigen-presenting cell function (*Sh2d1b1*) and synthesis of collagen III.

Clinical endomyocardial biopsies were modeled by performing transcript analyses on RNA isolated from the apex of the mouse cardiac allografts recovered on day 14 from recipients with high DSA titers, and compared gene expression in matched CAV lesions in a volcano plot (Figure 8B and Table 3). Like endomyocardial biopsies, these allograft apical tissue samples primarily contained interstitial infiltrates, myocardium, and small vessels. Expression of only two genes was up-regulated in the CAV

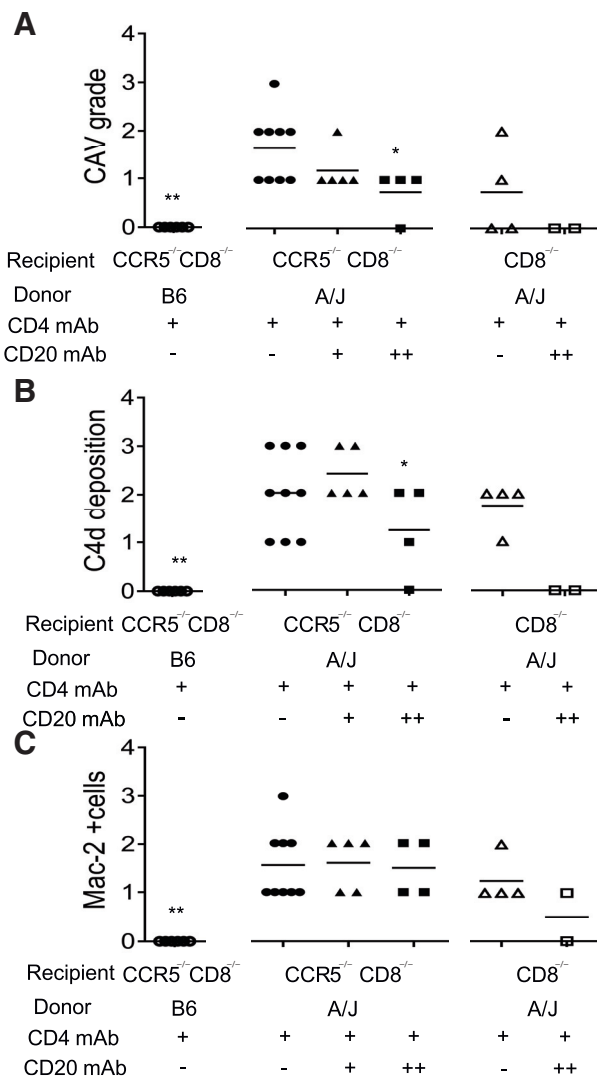


Figure 6 Histologic evaluation of cardiac isografts and allografts recovered from B6.CD8^{-/-} and B6.CCR5^{-/-}CD8^{-/-} recipients. Scoring of immunohistochemical staining of neointima for α -smooth muscle actin (A), C4d (B), and Mac2 (C) was performed in groups of heart grafts recovered on day 14 after transplant: B6 isografts to B6.CCR5^{-/-}CD8^{-/-} recipients; A/J allografts to B6.CCR5^{-/-}CD8^{-/-} recipients treated without or with two or three doses of anti-CD20 monoclonal antibody (mAb); and A/J allografts to B6.CD8^{-/-} recipients treated without or with three doses of anti-CD20 mAb. **P* < 0.05, ***P* < 0.01 versus A/J allografts to B6.CCR5^{-/-}CD8^{-/-} recipients treated with anti-CD4 mAb. CAV, cardiac allograft vasculopathy.

lesions versus the apical tissue, *Sele* (E-selectin) and *Tlr4*, but the apical tissue had 51 genes significantly up-regulated versus the CAV lesions. These up-regulated transcripts in the apical tissue included many involved with lymphocyte, dendritic cell, and myeloid cell activation, with leukocyte adhesion during cell-cell interactions and to matrix proteins, and with promotion of vascular development.

Discussion

CAV has been a major limitation to long-term patient survival from the beginning of clinical cardiac

transplantation.³⁰ Clinically, CAV is diagnosed by radiographic evidence of luminal narrowing in the coronary arteries. Histopathology of CAV in clinical samples has been confined to terminally rejected hearts explanted at the time of a second transplant or at autopsy because endomyocardial biopsies do not sample medium or large arteries.^{10,16,31} The fundamental pathologic finding in terminal CAV is a circumferential hyperplasia of the intima, composed of myofibrocytes and mononuclear leukocytes, leading to ischemic graft injury. In addition to intimal injury, chronic inflammation and fibrosis is frequently found in the adventitia. CAV often spares the medium, but in a minority of arteries, the medium is breached by transmural inflammation.³²

The pathologic heterogeneity of CAV has frequently been attributed to different underlying effector mechanisms. Previous experimental models have focused on CAV mediated by T cells. Chronic rejection is achieved in these models by performing transplants between strains with minimal antigenic differences that generate CD4 T-cell responses and little or no antibody responses.^{19–22} In these models, CAV develops in months and is characterized by high levels of IFN- γ -induced cytokines.²¹ More recently, DSA has been linked to the pathogenesis of CAV in humans.^{7,16} Therefore, we generated a model of CAV in which DSA titers could be calibrated to avoid acute rejection and generate different degrees of CAV. This was accomplished by using B6.CCR5^{-/-}CD8^{-/-} recipients that produce markedly higher titers of DSA than wild-type recipients. The antibody responses were delayed with a short course of anti-CD4 mAb to prevent acute rejection. To determine the effects of different levels of DSA, two regimens of anti-CD20 mAb were used to deplete B cells. These mouse models encompassed the heterogeneous manifestations of CAV. In heart allografts in B6.CCR5^{-/-}CD8^{-/-} recipients, the arterial pathology replicated cardinal features of CAV (namely, myofibrocytes that express α -smooth muscle actin and macrophages in an expanded intima). The neointima contained limited numbers of T cells because the recipients were CD8 deficient and were treated with anti-CD4 mAb. Intimal hyperplasia and luminal narrowing were most extensive in allografts from B6.CCR5^{-/-}CD8^{-/-} recipients producing high titers of DSA, and within this recipient group, DSA titers correlated with the incidence and severity of CAV. Consistent with this, recipient treatment with anti-CD20 antibodies to deplete B cells decreased DSA titers and the incidence and severity of CAV. In contrast to CAV in recipients producing high titers of DSA that included arterial occlusive neointimal expansion with macrophages and myofibrocytes expressing α -smooth muscle actin, transmural arteritis was a feature of CAV in allografts from B6.CD8^{-/-} recipients that produced low DSA titers, indicating different mechanisms of arterial pathology mediated with high versus low titers of DSA. There was considerable heterogeneity in the DSA titers induced in low, nondepleting anti-CD4 mAb-treated

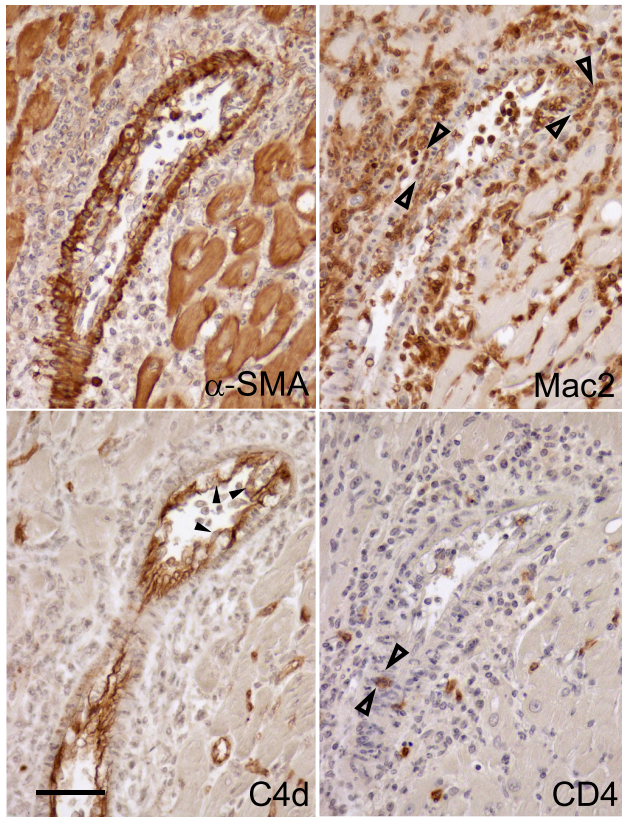


Figure 7 A/J cardiac allograft to B6.CD8^{-/-} recipient treated with three doses of antibodies to CD4 on days 0, 2, and 7 with arteritis 14 days after transplantation. Infiltration of the media by clusters of Mac2⁺ macrophages (open arrowheads) as well as intense interstitial and periarterial infiltrates of macrophages were evident. Occasional CD4 T cells also breach the media. C4d stains demonstrate extensive endothelial cell injury in the artery (closed arrowheads) and capillaries. Scale bar = 50 μm. α-SMA, α-smooth muscle actin.

B6.CCR5^{-/-}CD8^{-/-} recipients of heart allografts. It is likely that the range of DSA titers is due to differences in the impact of the anti-CD4 mAb on the recipient CD4 T cells as well as the early time after transplant that the allografts were recovered for analysis. Consistent with these findings, recent reports underline the value of post-transplant assessment of DSA titer for transplant recipient risk stratification for development of CAV and allograft loss.^{2,33,34} Higher DSA mean fluorescence intensity levels correlate with the capacity to activate complement and are associated with development of transplant vasculopathy and allograft loss.^{35–37} Antibody titer affects the ability of human leukocyte antigen DSA to transduce signals and subsequent endothelial activation. In previous work, increasing quantities of human leukocyte antigen antibody binding to endothelial cells were found to result in augmented fibroblast growth factor receptor (FGFR) expression and cellular proliferation and migration.^{12,38} In contrast, lower antibody concentrations trigger signal transduction pathways that up-regulate prosurvival genes and antiapoptotic proteins in endothelial cells.³⁹

Molecular interrogation of cardiac transplant rejection has been primarily limited to endomyocardial biopsies in humans and homogenates of whole heart grafts in small animal models.¹⁷ The major sources of RNA in these samples are interstitial infiltrates, myocardium, and small vessels. However, CAV is predominantly a lesion of coronary arteries. Our model of CAV allows probing of early transcriptome signatures in microdissected large arteries from mouse cardiac allografts. It was somewhat surprising that the number of transcripts up-regulated and down-regulated in arterial lesions in allografts from recipients with high versus low titers of DSA was small. Transcriptomic analysis identified the Notch ligand *Dll4* as the most elevated transcript in CAV associated with high versus low titers of DSA. *Dll4* was discovered as a differentially expressed gene in arterial endothelium.⁴⁰ Up-regulation of *Dll4* has been reported in endomyocardial biopsies from human cardiac transplants during antibody-mediated rejection.⁴¹ *In vitro* co-culture studies indicate that *Dll4* is up-regulated by both endothelial cells and monocytes, and that *Dll4* induces macrophage polarization toward an inflammatory phenotype.⁴¹ In support of this, mouse models of atherosclerosis indicate macrophage stimulation through *Dll4* induces a proinflammatory profile.⁴² Other transcripts up-regulated during the antibody-mediated CAV included those involved with cell differentiation (*Abi1*), those mediating cell spreading on endothelial basement membranes (*Cspg4*), and those associated with inflammatory immune cell functions (*Nfatc2*) and expressed by heart-resident macrophages during inflammatory processes (*Trem2*).⁴³ Intriguingly, the integrin α subunit *Itga6* was also increased in CAV, and its partner integrin $\beta 4$ was previously shown to form a complex with MHC and is required for proliferation of endothelial cells stimulated by MHC class I-specific antibodies.¹⁵ In contrast, allografts from B6.CCR5^{-/-}CD8^{-/-} recipients treated with B-cell-depleting antibodies had increased arterial expression of genes encoding chemoattractants for T cells and dendritic cells and genes involved in antigen presentation. Expression of these genes could explain the greater infiltration and activation of macrophages and T cells in the media of arteries of allografts from B6.CD8^{-/-} recipients, which produced low titers of DSA. One limitation of the approach used in the current studies is the limited number of genes probed, but the code set used includes >700 probes for inflammatory mediators. It is likely that extension of these studies to single-cell sequencing of the arterial lesions will identify other transcripts expressed during DSA-induced CAV that are not represented in the probe set used in these studies.

Clinical endomyocardial biopsies were modeled by performing transcript analyses on RNA isolated from the apex of the mouse cardiac allografts. Like endomyocardial biopsies, these tissue samples primarily contained interstitial infiltrates, myocardium, and small vessels. Histologic evaluation of the myocardium confirmed an increased interstitial

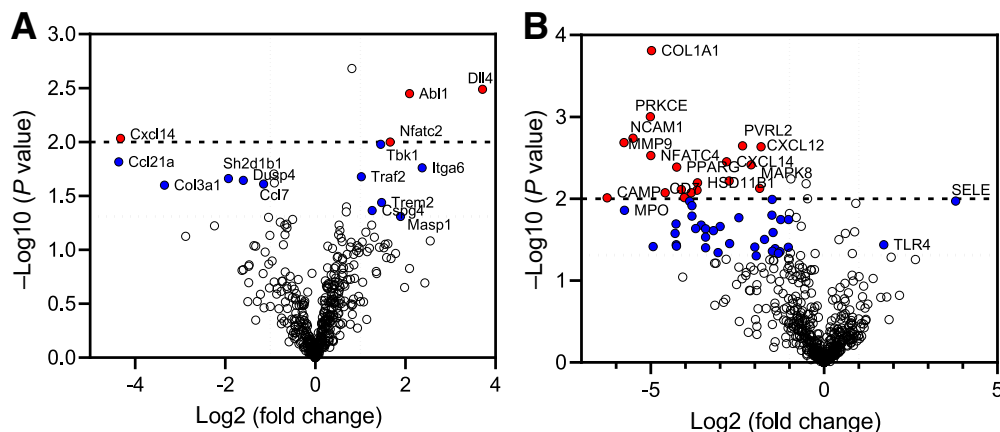


Figure 8 Volcano plots of multiplexed RNA detection indicate increased and decreased genes expressed in A/J heart allografts on day 14 after transplant between: microdissected graft arteries with cardiac allograft vasculopathy (CAV) from B6.CCR5^{-/-}CD8^{-/-} recipients versus graft arteries from B6.CCR5^{-/-}CD8^{-/-} recipients treated with anti-mouse CD20 monoclonal antibody to deplete B cells (**A**); and CAV lesions compared with intact apical wall of A/J allografts in B6.CCR5^{-/-}CD8^{-/-} recipients (**B**). In both volcano plots, open gray circles represent transcripts that are not changed between the two groups; solid blue circles indicate differentially expressed genes (DEGs) with $P < 0.05$; solid red circles indicate DEGs with $P < 0.01$. The most highly significant DEGs are labeled on the plots. The **higher dashed horizontal line** indicates the cutoff for differentially expressed transcripts with a $P < 0.01$, and the **lower dotted horizontal line** indicates the cutoff for differentially expressed transcripts with a $P < 0.05$.

fibrosis in the myocardium. However, this pathologic process is more global and not directly related to the mechanisms that cause CAV in large arteries. Expression of only E-selectin and toll-like receptor 4 was up-regulated in the DSA-mediated CAV lesions versus the apical tissue, but the apical tissue had 51 genes significantly up-regulated versus the CAV lesions. The up-regulated transcripts in the apical tissue included many promoting lymphocyte, dendritic cell, and myeloid cell recruitment and activation, myocardial ischemia, and vascular development. One of the most highly up-regulated genes was for myeloperoxidase, which Swirski et al²⁰ have localized by magnetic resonance imaging to the ventricular wall rather than coronary arteries. Transcripts related to T-cell-mediated CAV in a mouse minor antigen disparate model are also compartmentalized to large arteries and not reflected in the surrounding myocardial tissues.²¹

Interestingly, high expression of *Tlr4* is observed in CAV lesions in both the DSA- and the T-cell-mediated injury responses. These results reveal transcriptional differences between anatomic regions of the heart, but the apical myocardial transcriptional signature remains to be distinguished from grafts without CAV.

Recent studies have indicated the expression of genes associated with natural killer cell activation in biopsies of clinical kidney and heart grafts during acute antibody-mediated rejection.^{44,45} This identification has resulted in a panel of six natural killer cell activation associated transcripts that are markers of this pathology. The expression of three of these genes associated with natural killer cell activation during antibody-mediated rejection was tested in the RNA isolated from the apex of the heart allografts by real-time quantitative PCR. *Mybl1*, *SH2D1B*, and *CX3CR1* were

Table 2 Consensus Differentially Expressed Genes by Rosalind and nCounter Analysis for CAV Lesions in Recipients with High versus Low DSA

Increased in high DSA CAV				Decreased in high DSA CAV			
Rosalind		nCounter		Rosalind		nCounter	
Genes	Log2 fold change	Genes	Log2 fold change	Genes	Log2 fold change	Genes	Log2 fold change
<i>Dll4</i>	4.33	<i>Dll4</i>	3.71	<i>Ccl21a</i>	-4.55	<i>Ccl21a</i>	-4.36
<i>Itga6</i>	2.33	<i>Itga6</i>	2.37	<i>Cxcl14</i>	-4.3	<i>Cxcl14</i>	-4.32
<i>Abl1</i>	2.05	<i>Abl1</i>	2.09	<i>Col3a1</i>	-3.41	<i>Col3a1</i>	-3.35
<i>Masp1</i>	1.8	<i>Masp1</i>	1.89	<i>Sh2d1b1</i>	-1.97	<i>Sh2d1b1</i>	-1.93
<i>Nfatc2</i>	1.62	<i>Nfatc2</i>	1.66	<i>Dusp4</i>	-1.64	<i>Dusp4</i>	-1.6
<i>Trem2</i>	1.47	<i>Trem2</i>	1.47	<i>Ccl7</i>	-1.18	<i>Ccl7</i>	-1.15
<i>Tbk1</i>	1.41	<i>Tbk1</i>	1.45				
<i>Cspg4</i>	1.21	<i>Cspg4</i>	1.26				

CAV, cardiac allograft vasculopathy; DSA, donor-specific antibody.

Table 3 Consensus Differentially Expressed Genes by Rosalind and nCounter Analysis for CAV Lesions versus Apex in Recipients with High DSA

Increased in CAV versus apex				Decreased in CAV versus apex			
Rosalind		nCounter		Rosalind		nCounter	
Genes	Log2 fold change	Genes	Log2 fold change	Genes	Log2 fold change	Genes	Log2 fold change
<i>Sele</i>	3.8	<i>Sele</i>	3.64	<i>Camp</i>	-6.26	<i>Camp</i>	-6.13
<i>Tlr4</i>	1.72	<i>Tlr4</i>	1.65	<i>Mmp9</i>	-5.77	<i>Mmp9</i>	-5.33
				<i>Mpo</i>	-5.75	<i>Mpo</i>	-5.31
				<i>Ncam1</i>	-5.51	<i>Ncam1</i>	-5.55
				<i>Prkce</i>	-5.01	<i>Prkce</i>	-4.57
				<i>Nftatc4</i>	-5.00	<i>Nftatc4</i>	-4.56
				<i>Cola1a</i>	-4.98	<i>Cola1a</i>	-5.05
				<i>Bcl6</i>	-4.93	<i>Bcl6</i>	-5.01
				<i>Cd7</i>	-4.58	<i>Cd7</i>	-4.14

CAV, cardiac allograft vasculopathy; DSA, donor-specific antibody.

expressed at high levels in the heart allografts but not iso-grafts (data not shown). However, the expressions of all three genes were observed in allografts regardless of high versus low DSA titers and development of CAV. Consistent with these results, NanoString analyses indicated expression of *SH2D1B* was higher in dissected allograft arteries from B6.CCR5^{-/-}CD8^{-/-} recipients treated with anti-CD20 mAb than in allograft arteries from control-treated recipients (Figure 7).

In summary, the current experiments established a mouse model of DSA-mediated CAV that allows selective probing of the arteries during the development of CAV and provides mechanistic insights to the pathogenesis of CAV. This approach identified expression of specific transcripts within the arterial CAV lesion that were not detected by testing RNA isolated from the unselective homogenates of graft tissue. The development of this pathology can be further interrogated by performing arterial dissection and molecular analysis on grafts from recipients at different times in the progression of antibody responses to MHC class I and II antigens. Furthermore, the model will allow manipulation to begin testing the function of allograft- and recipient-derived cells in the development of the arterial CAV lesions.

Acknowledgment

We thank John W. Peterson, Ph.D. (Lerner Imaging Core), for expert assistance with the Leica LMD7000 laser microdissection microscope.

Supplemental Data

Supplemental material for this article can be found at <http://doi.org/10.1016/j.ajpath.2022.04.003>.

References

- Chih S, Chong AY, Mielniczuk LM, Bhatt DL, Beanlands RS: Allograft vasculopathy: the Achilles' heel of heart transplantation. *J Am Coll Cardiol* 2016, 68:80–91
- Loupy A, Coutance G, Bonnet G, Van Keer J, Raynaud M, Aubert O, Bories MC, Racape M, Yoo D, Duong Van Huyen JP, Bruneval P, Taupin JL, Lefaucheur C, Varnous S, Leprince P, Guillemain R, Empana JP, Levine R, Naesens M, Patel JK, Jouven X, Kobashigawa J: Identification and characterization of trajectories of cardiac allograft vasculopathy after heart transplantation: a population-based study. *Circulation* 2020, 141:1954–1967
- Lund LH, Edwards LB, Dipchand AI, Goldfarb S, Kucheryavaya AY, Levvey BJ, Meiser B, Rossano JW, Yusem RD, Stehlik J, International Society for Heart and Lung Transplantation: The Registry of the International Society for Heart and Lung Transplantation: thirty-third adult heart transplantation report-2016; focus theme: primary diagnostic indications for transplant. *J Heart Lung Transplant* 2016, 35:1158–1169
- Jansen MA, Otten HG, de Weger RA, Huibers MM: Immunological and fibrotic mechanisms in cardiac allograft vasculopathy. *Transplantation* 2015, 99:2467–2475
- Lee F, Nair V, Chih S: Cardiac allograft vasculopathy: insights on pathogenesis and therapy. *Clin Transplant* 2020, 34:e13794
- Frank R, Molina MR, Goldberg LR, Wald JW, Kamoun M, Lal P: Circulating donor-specific anti-human leukocyte antigen antibodies and complement C4d deposition are associated with the development of cardiac allograft vasculopathy. *Am J Clin Pathol* 2014, 142:809–815
- Loupy A, Toquet C, Rouvier P, Beuscart T, Bories MC, Varnous S, Guillemain R, Pattier S, Suberbielle C, Leprince P, Lefaucheur C, Jouven X, Bruneval P, Duong Van Huyen JP: Late failing heart allografts: pathology of cardiac allograft vasculopathy and association with antibody-mediated rejection. *Am J Transplant* 2016, 16:111–120
- Ticehurst EH, Molina MR, Frank R, Kearns J, Lal P, Goldberg LR, Tsai D, Wald J, Kamoun M: Antibody-mediated rejection in heart transplant patients: long-term follow up of patients with high levels of donor-directed anti-DQ antibodies. *Clin Transpl* 2011, 43:409–414
- Valenzuela NM, Reed EF: Antibody-mediated rejection across solid organ transplants: manifestations, mechanisms, and therapies. *J Clin Invest* 2017, 127:2492–2504
- Wehner JR, Fox-Talbot K, Halushka MK, Ellis C, Zachary AA, Baldwin WM 3rd: B cells and plasma cells in coronaries of chronically rejected cardiac transplants. *Transplantation* 2010, 89:1141–1148

11. Jin YP, Valenzuela NM, Zhang X, Rozengurt E, Reed EF: HLA class II-triggered signaling cascades cause endothelial cell proliferation and migration: relevance to antibody-mediated transplant rejection. *J Immunol* 2018, 200:2372–2390
12. Jindra PT, Hsueh A, Hong L, Gjertson D, Shen XD, Gao F, Dang J, Mischel PS, Baldwin WM 3rd, Fishbein MC, Kupiec-Weglinski JW, Reed EF: Anti-MHC class I antibody activation of proliferation and survival signaling in murine cardiac allografts. *J Immunol* 2008, 180:2214–2224
13. Michaels PJ, Espejo ML, Kobashigawa J, Alejos JC, Burch C, Takemoto S, Reed EF, Fishbein MC: Humoral rejection in cardiac transplantation: risk factors, hemodynamic consequences and relationship to transplant coronary artery disease. *J Heart Lung Transplant* 2003, 22:58–69
14. Salehi S, Sosa RA, Jin YP, Kageyama S, Fishbein MC, Rozengurt E, Kupiec-Weglinski JW, Reed EF: Outside-in HLA class I signaling regulates ICAM-1 clustering and endothelial cell-monocyte interactions via mTOR in transplant antibody-mediated rejection. *Am J Transplant* 2018, 18:1096–1109
15. Valenzuela NM, Mulder A, Reed EF: HLA class I antibodies trigger increased adherence of monocytes to endothelial cells by eliciting an increase in endothelial P-selectin and, depending on subclass, by engaging FcγRs. *J Immunol* 2013, 190:6635–6650
16. Wehner J, Morrell CN, Reynolds T, Rodriguez ER, Baldwin WM 3rd: Antibody and complement in transplant vasculopathy. *Circ Res* 2007, 100:191–203
17. Wei X, Valenzuela NM, Rossetti M, Sosa RA, Nevarez-Mejia J, Fishbein GA, Mulder A, Dhar J, Keslar KS, Baldwin WM 3rd, Fairchild RL, Hou J, Reed EF: Antibody-induced vascular inflammation skews infiltrating macrophages to a novel remodeling phenotype in a model of transplant rejection. *Am J Transplant* 2020, 20:2686–2702
18. Zhang X, Rozengurt E, Reed EF: HLA class I molecules partner with integrin beta4 to stimulate endothelial cell proliferation and migration. *Sci Signal* 2010, 3:ra85
19. Sayegh MH, Wu Z, Hancock WW, Langmuir PB, Mata M, Sandner S, Kishimoto K, Sho M, Palmer E, Mitchell RN, Turka LA: Allograft rejection in a new allospecific CD4+ TCR transgenic mouse. *Am J Transplant* 2003, 3:381–389
20. Swirski FK, Wildgruber M, Ueno T, Figueiredo JL, Panizzi P, Iwamoto Y, Zhang E, Stone JR, Rodriguez E, Chen JW, Pittet MJ, Weissleder R, Nahrendorf M: Myeloperoxidase-rich Ly-6C+ myeloid cells infiltrate allografts and contribute to an imaging signature of organ rejection in mice. *J Clin Invest* 2010, 120:2627–2634
21. Kaul AM, Goparaju S, Dvorina N, Iida S, Keslar KS, de la Motte CA, Valujskikh A, Fairchild RL, Baldwin WM 3rd: Acute and chronic rejection: compartmentalization and kinetics of counterbalancing signals in cardiac transplants. *Am J Transplant* 2015, 15:333–345
22. Millrain M, Scott D, Addey C, Dewchand H, Ellis P, Ehrmann I, Mitchell M, Burgoyne P, Simpson E, Dyson J: Identification of the immunodominant HY H2-D(k) epitope and evaluation of the role of direct and indirect antigen presentation in HY responses. *J Immunol* 2005, 175:7209–7217
23. Hirohashi T, Uehara S, Chase CM, DellaPelle P, Madsen JC, Russell PS, Colvin RB: Complement independent antibody-mediated endarteritis and transplant arteriopathy in mice. *Am J Transplant* 2010, 10:510–517
24. Lin CM, Gill RG, Mehrad B: The natural killer cell activating receptor, NKG2D, is critical to antibody-dependent chronic rejection in heart transplantation. *Am J Transplant* 2021, 21:3550–3560
25. Abe T, Su CA, Iida S, Baldwin WM 3rd, Nonomura N, Takahara S, Fairchild RL: Graft-derived CCL2 increases graft injury during antibody-mediated rejection of cardiac allografts. *Am J Transplant* 2014, 14:1753–1764
26. Nozaki T, Amano H, Bickerstaff A, Orosz CG, Novick AC, Tanabe K, Fairchild RL: Antibody-mediated rejection of cardiac allografts in CCR5-deficient recipients. *J Immunol* 2007, 179:5238–5245
27. Gorbacheva V, Fan R, Beavers A, Fairchild RL, Baldwin WM 3rd, Valujskikh A: Anti-donor MHC class II alloantibody induces glomerular injury in mouse renal allografts subjected to prolonged cold ischemia. *J Am Soc Nephrol* 2019, 30:2413–2425
28. Murata K, Fox-Talbot K, Qian Z, Takahashi K, Stahl GL, Baldwin WM 3rd, Wasowska BA: Synergistic deposition of C4d by complement-activating and non-activating antibodies in cardiac transplants. *Am J Transplant* 2007, 7:2605–2614
29. Clausell N, Butany J, Gladstone P, Lonn E, Liu P, Cardella C, Feindel C, Daly PA: Myocardial vacuolization, a marker of ischemic injury, in surveillance cardiac biopsies posttransplant: correlations with morphologic vascular disease and endothelial dysfunction. *Cardiovasc Pathol* 1996, 5:29–37
30. Rider AK, Copeland JG, Hunt SA, Mason J, Specter MJ, Winkle RA, Bieber CP, Billingham ME, Dong E Jr, Griep RB, Schroeder JS, Stinson EB, Harrison DC, Shumway NE: The status of cardiac transplantation, 1975. *Circulation* 1975, 52:531–539
31. Lu WH, Palatnik K, Fishbein GA, Lai C, Levi DS, Perens G, Alejos J, Kobashigawa J, Fishbein MC: Diverse morphologic manifestations of cardiac allograft vasculopathy: a pathologic study of 64 allograft hearts. *J Heart Lung Transplant* 2011, 30:1044–1050
32. Tellides G, Pober JS: Inflammatory and immune responses in the arterial media. *Circ Res* 2015, 116:312–322
33. Olymbios M, Kobashigawa JA: Crossing low-level donor-specific antibodies in heart transplantation. *Curr Opin Organ Transplant* 2019, 24:227–232
34. Wang M, Patel NJ, Zhang X, Kransdorf EP, Azarbal B, Kittleson MM, Czer LSC, Kobashigawa JA, Patel JK: The effects of donor-specific antibody characteristics on cardiac allograft vasculopathy. *Clin Transplant* 2021, 35:e14483
35. Das BB, Lacelle C, Zhang S, Gao A, Fixler D: Complement (C1q) binding de novo donor-specific antibodies and cardiac-allograft vasculopathy in pediatric heart transplant recipients. *Transplantation* 2018, 102:502–509
36. Gloor JM, Winters JL, Cornell LD, Fix LA, DeGoey SR, Knauer RM, Cosio FG, Gandhi MJ, Kremers W, Stegall MD: Baseline donor-specific antibody levels and outcomes in positive crossmatch kidney transplantation. *Am J Transplant* 2010, 10:582–589
37. Viglietti D, Loupy A, Vernerey D, Bentelejewski C, Gosset C, Aubert O, Duong van Huyen JP, Jouven X, Legendre C, Glotz D, Zeevi A, Lefaucheur C: Value of donor-specific anti-HLA antibody monitoring and characterization for risk stratification of kidney allograft loss. *J Am Soc Nephrol* 2017, 28:702–715
38. Jindra PT, Zhang X, Mulder A, Claas F, Veale J, Jin YP, Reed EF: Anti-HLA antibodies can induce endothelial cell survival or proliferation depending on their concentration. *Transplantation* 2006, 82:S33–S35
39. Jin YP, Fishbein MC, Said JW, Jindra PT, Rajalingam R, Rozengurt E, Reed EF: Anti-HLA class I antibody-mediated activation of the PI3K/Akt signaling pathway and induction of Bcl-2 and Bcl-xL expression in endothelial cells. *Hum Immunol* 2004, 65:291–302
40. Shutter JR, Scully S, Fan W, Richards WG, Kitajewski J, Deblandre GA, Kintner CR, Stark KL: Dll4, a novel Notch ligand expressed in arterial endothelium. *Genes Dev* 2000, 14:1313–1318
41. Pabois A, Pagie S, Gerard N, Labois C, Pattier S, Hulin P, Nedellec S, Toquet C, Charreau B: Notch signaling mediates crosstalk between endothelial cells and macrophages via Dll4 and IL6 in cardiac microvascular inflammation. *Biochem Pharmacol* 2016, 104:95–107

42. Nakano T, Fukuda D, Koga J, Aikawa M: Delta-like ligand 4-Notch signaling in macrophage activation. *Arterioscler Thromb Vasc Biol* 2016, 36:2038–2047
43. Bajpai G, Schneider C, Wong N, Bredemeyer A, Hulsmans M, Nahrendorf M, Eelman S, Kreisel D, Liu Y, Itoh A, Shankar TS, Selzman CH, Drakos SG, Lavine KJ: The human heart contains distinct macrophage subsets with divergent origins and functions. *Nat Med* 2018, 24:1234–1245
44. Halloran PF, Potena L, Van Huyen JD, Bruneval P, Leone O, Kim DH, Jouven X, Reeve J, Loupy A: Building a tissue-based molecular diagnostic system in heart transplant rejection: the heart Molecular Microscope Diagnostic (MMDx) System. *J Heart Lung Transplant* 2017, 36:1192–1200
45. Loupy A, Duong Van Huyen JP, Hidalgo L, Reeve J, Racape M, Aubert O, Venner JM, Falmuski K, Bories MC, Beuscart T, Guillemain R, Francois A, Pattier S, Toquet C, Gay A, Rouvier P, Varnous S, LePrince P, Empana JP, Lefaucheur C, Bruneval P, Jouven X, Halloran PF: Gene expression profiling for the identification and classification of antibody-mediated heart rejection. *Circulation* 2017, 135:917–935